Preprints of the 21st IFAC World Congress (Virtual)
Berlin, Germany, July 12-17, 2020

Design of a Robust Fractional Order Controller for Burning Zone Temperature Control in an Industrial Cement Rotary Kiln

V. Feliu-Batlle*, R. Rivas-Perez*

**Escuela Técnica Superior de Ingenieros Industriales and Instituto de Investigaciones Energéticas y Aplicaciones Industriales, Universidad de Castilla-La Mancha, Campus Universitario s/n, Ciudad Real, 13071, Spain (e-mail: vicente.feliu@uclm.es).*
***Department of Automatica and Computer Science, Universidad Tecnológica de la Habana CUJAE, Calle 114 No 11901, Marianao, Habana, 19390, Cuba (e-mail:rivas@automatica.cujae.edu.cu)*

Abstract: The control of the temperature of the burning zone of an industrial cement rotary kiln is addressed in this paper. An experimental identification of the process was carried out, which yielded a second order transfer function with no zeros but with a very large time delay. Moreover, it was detected that this time delay could change between ±8% of its nominal value. Then a robust controller had to be designed for this process. A standard *PI* controller, a *PI* controller embedded in a Smith Predictor scheme, and a fractional-order controller embedded in a Smith Predictor have been studied. A method to design the fractional-order controller is developed in this paper that yields better results than the other studied controllers. Simulated results are presented.

Keywords: Fractional order controller, robust control, time-varying time delay, cement rotary kiln, burning zone temperature, control oriented model

1. INTRODUCTION

The cement industry is currently a fundamental factor for economic and social development worldwide, because it represents the cornerstone of the construction sector (Schneider, 2019). The cement is the most used building material on a global scale, and it is a key element for the development and economic growth of any country. The cement production involves several complex processes that take place under different raised temperatures. Consequently, the cement industry is one of the industries with the highest thermal energy consumption in the world, represents about 5% of global anthropogenic CO_2 emissions, and affects the environment, the depletion of natural resources, as well as the health and safety of people (Atmaca and Yumrutas, 2014).

The cement is obtained from the clinker pulverizing, which is its main component and it is attained from a burned mixture of clay and limestone materials (raw meal), adding it grinded gypsum (Alsop, 2014). The clinker production process is the stage of highest energy consumption in the cement industry, representing approximately 80% of the total thermal energy consumed (Atmaca and Yumrutas, 2014). Therefore, research aimed at ensuring the quality clinker production and reducing energy consumption and CO_2 emissions to the environment by applying modern manufacturing and control methods is of great scientific-technical interest and represents a huge challenge for the international scientific community.

The clinker production process (clinkerization) is performed in the rotary kilns, which are the most important units of the cement industry and develop four different functions: 1) chemical reactor, 2) heat generator 3) heat exchanger, and 4) conveyor of gases and solids (Alsop, 2014). The main objective of these kilns is to produce clinker of consistent quality from raw meal with minimum energy consumption.

In the dry cement process lines, the rotary kilns are divided into three zones: heating zone, burning zone, and cooling zone. In the burning zone, at a nominal operating temperature of 1450ºC, a chemical reaction takes place that makes it possible to obtain the tricalcium silicate, which is the main component of clinker and which confers the mechanical resistance characteristic. The burning zone temperature (*BZT*) is a key technological variable that must be controlled to ensure the clinker quality with the minimum energy consumption. Therefore, it is vital to maintain the nominal operating *BZT* and avoid its fluctuations (Chen et al., 2016).

However, the control of the *BZT* is not a simple task due to the complex dynamic behavior of this process that is characterized by exhibiting non-linear and distributed parameters, as well as large time-varying time delays due to changing raw meal characteristics, and both physical and chemical reactions that happen in the burning zone (Ravi et al., 2016).

Currently, the most commonly used procedures to control of the *BZT* are: 1) manual control by means of human operators with expert knowledge of the process, and 2) conventional *PID* control. However, it is well known that these control procedures are not sufficient when the processes are characterized by distributed dynamic parameters and a time-varying time delay (Astrom and Hagglund, 2009; Feliu-Batlle and Rivas-Perez, 2019). Therefore, the quality of the obtained clinker is unstable, it does not reach the required international standards and the energy consumption is high. To solve these

*This work has been supported in part by the University of Castilla-La Mancha under Project 2019-GRIN-26969 and in part by the European Social Fund (FEDER, EU).

drawbacks, different control strategies have been proposed in the last two decades to control the *BZT*, which include: model predictive control (Salcedo et al., 2018), fuzzy control (Zhang, 2017), artificial neural network control (Ying, 2014), and neuro-fuzzy control (Fallahpour et al., 2008). However, these controllers require a very precise knowledge of the dynamic behavior of the cement rotary kiln, which is usually something challenging to be obtained due to the dynamic complexity of the physical and chemical reactions involved. Moreover, they do not consider the large time-varying time delay of this process that makes significantly difficult the effective control of the *BZT*. Then robust controllers are required for the effective control of the *BZT*, in order to achieve the established international standard of clinker quality with the minimum energy consumption. This issue has been insufficiently addressed in the scientific literature.

Fractional order controllers have been proposed for robust control of processes with complex dynamical behaviors, e.g. Monje et al., 2010; Sayyaf and Tavazoei, 2018. These controllers have more tuning parameters than standard controllers. It enables them to increase their robustness against time-varying dynamic parameters of the processes. Moreover, their structure is simpler than the one of other robust controllers, and their implementation is relatively easy.

Based on these considerations, our objective is to design a robust fractional order controller for effective control of the *BZT* in an industrial cement rotary kiln. The main contributions of this paper are the development of a new mathematical model of a *BZT* with a time-varying time delay, and a new methodology to design a fractional order controller for robust control of the *BZT* in cement rotary kilns.

The organization of the paper is as follows. This section has provided the introduction to *BZT* control in cement rotary kilns. Section 2 introduces the cement rotary kiln under study and, based on a system identification procedure, obtains a linear model with time-varying time delay of a *BZT*. Section 3 develops the fractional-order controller and compares it with other controllers. Section 4 gives some conclusions.

2. SYSTEM IDENTIFICATION OF BURNING ZONE TEMPERATURE

In the current study, the René Arcay cement factory of the Mixed Company Cementos Curazao S.A. at the municipality of Mariel, Cuba, is considered. The cement factory operates on a dry cement process line. The rotary kiln is a refractory steel cylindrical tunnel with a length of 93.6 meters and a diameter of 4.6 meters. The kiln has a slight slope of 4° and slowly rotates on its axis at 2.0-3.0 rpm by an electrical motor with a working power of 283 kW. At the lower end of the kiln, a fuel burner is installed to ensure temperatures over the 1400°C in the burning zone. The average clinker production capacity of the kiln is about 2200 t/day. The kiln has a four-stage cyclone preheater to heat the raw meal before it enters the kiln, by using the hot gases from the burning zone.

Raw meal is fed into the upper end of the kiln and the rotation of the kiln causes it to move gradually towards the outfeed side with a variable residence time between 40 and 60 minutes. Upon reaching the combustion zone, the raw meal attains the nominal operating temperature of about 1450°C, causing the chemical reactions that transform it into clinker. After leaving the combustion zone, the clinker is quickly cooled to 1000°C in order to avoid the reversion of the produced chemical reactions. This abrupt cooling is also necessary to improve clinker quality and for heat recovery. A scheme of the studied cement rotary kiln is shown in Fig. 1.

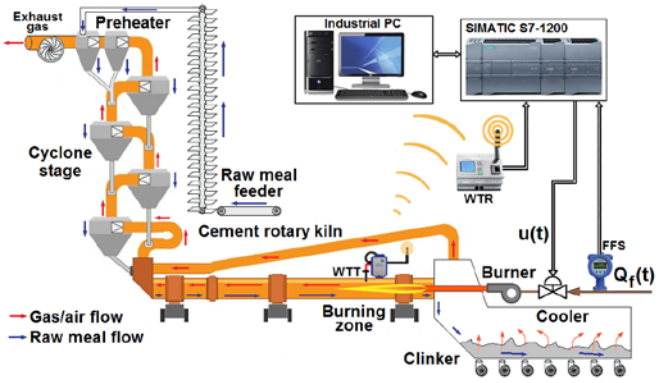

Fig. 1. Schematic of the cement rotary kiln under study.

This cement rotary kiln can operate manually or automatically, has a medium level of automation, the quality of the clinker obtained is unstable, and has high fuel consumption. Therefore, its modernization is planned in order to improve its performance.

The kiln is equipped with the following instruments: wireless temperature transmitter (*WTT*) and receiver (*WTR*), fuel flow sensor (*FFS*), fuel control valve, a *PLC SIMATIC S7-1200*, an industrial personal computer (*PC*), etc. The *WTT* is installed on the external surface of the rotary kiln and it obtains the temperature data by means of a thermocouple installed inside the kiln. It has a mechanical protection cover that attenuates the heat irradiation of the kiln surface. The *WTT* sends real time data to a *WTR* installed in the control room of the rotary kiln. The industrial *PC* has a *SCADA* application installed that performs the supervision of the kiln operation.

Despite the cement rotary kiln is well known as a complex distributed parameter system (Zhou and Meng, 2014), it is not necessary to know the temperature variations along the whole cement rotary kiln in order to carry out the *BZT* control, but only at a specific measurement point (Salcedo et al., 2018). Thus, a linear model with lumped parameters and a time delay can adequately characterize the dynamical behavior of a *BZT* at a specific point (Chen et al., 2016). This model can therefore be obtained by using system identification techniques, which are experimental procedures based on real-time input and output operation data derived from the process under study. Because the kiln object of this study is a real industrial cement rotary kiln subject to operation and safety restrictions, the system identification experiments to obtain the operation data cannot be developed based on the response to a persistently exciting binary signal input (e.g. a *PRBS*). Therefore, with this purpose a step like input signal was used. This signal excites the dynamics of interest and can be easily generated. By limiting its amplitude, it is possible to keep the process within its nominal operation regime allowing the

attainment of simple control-oriented models with an acceptable degree of accuracy (Ljung, 1999).

In our experimental identification of the process based on a step like input, the fuel flowrate ($Q_f(t)$) was considered the input variable $u(t)$, and the burning zone temperature the output variable $y(t)$. The most important disturbances that influence this process are the variation in the raw meal load, and its water and material contents, that cause great fluctuations in the burner flame and originate abrupt variations in the temperature of the burning zone (Chen et al., 2016). Fig. 1 shows the experimental arrangement made for the collection of input/output data under the nominal operating regime of the studied kiln. The experiment based on the response to a step like input consisted of increasing the fuel flowrate entering the kiln burner by 11.62% (from 8600 to 9600 l/h) and measuring the temperature variation in the combustion zone of the kiln. The experimental response obtained is shown in Fig. 2.

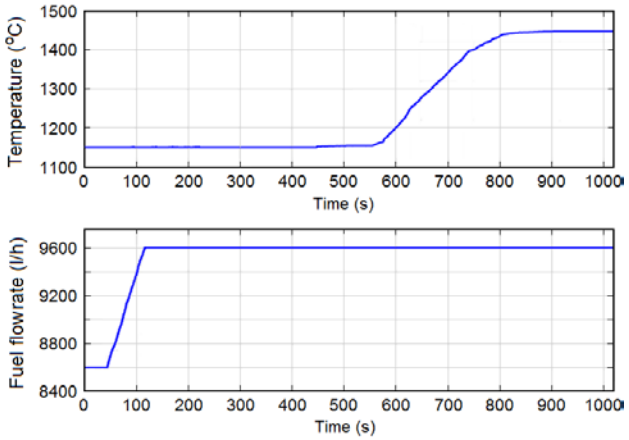

Fig. 2. Experimental response of *BZT* to a step like input.

From Fig. 2 it is observed that the *BZT* varies from 1150ºC to its nominal operating value of 1450ºC in an overall time period of 800 s. The shape of the response suggests that the nominal dynamic behavior of the *BZT* can be represented by a second order transfer function with a dominant time delay given by:

$$P(s)=\frac{K}{(T_1\cdot s+1)(T_2\cdot s+1)}e^{-\tau\cdot s}=G(s)\cdot e^{-\tau\cdot s}\ , \qquad (1)$$

where K is the static gain, T_1 and T_2 are time constants, τ is the time delay, and $G(s)$ is the rational part of $P(s)$. The estimated parameters of the nominal model $P_0(s)$ are: $K_0=0.3$ºC·h/l, $T_{10}=55.39$ s, $T_{20}=43.29$ s, and $\tau_0=500$ s. The cross-validation result of $P_0(s)$ was quantified by a *FIT* index (Ljung, 1999) of 90.47%. Since this index is higher than 80%, which is the minimum index value considered valid, the obtained model $P_0(s)$ can be regarded as accurate enough to be used in the controller design (Ljung, 1999). The settling time of the step response of $G_0(s)$ is 235 s and the settling time of $P_0(s)$ is $t_{s0,open}=235+\tau_0=735$ s.

The experiments developed in the *BZT* of our cement rotary kiln proved that the higher the water content in the raw meal is, the greater the *BZT* time delay would be. It is due to the fact that for a given raw meal load, if its water content rises, more heating time is required to evaporate this water and, therefore, to observe growths in the *BZT*. These experiments evidenced that model (1) of the *BZT* has a time-varying time delay included in the following range:

$$\tau\in[\tau_-,\tau_+]=[460,\ 540]. \qquad (2)$$

Consequently, for an effective control of our *BZT*, the design of a robust controller is needed.

3. DESIGN OF A ROBUST FRACTIONAL-ORDER CONTROLLER FOR OUR *BZT*

3.1 Partial cancellation of the dynamics

It is well known that $G_0(s)$ can be approximated by:

$$G_0(s)=\frac{K_0}{(T_{10}\cdot s+1)(T_{20}\cdot s+1)}\approx\frac{K_0}{(T_{10}+T_{20})\cdot s+1}=G_c(s)$$

in a certain range $\omega\in[0,\ \omega_{\max}]$ of the frequency response. Let us consider this approximation valid in the frequency range in which the magnitude of the Bode diagram of $G_0(s)/G_c(s)$ is less than ±1 db, and the phase diagram is less than $\pm5^\circ$. Fig. 3 shows these diagrams and these accuracy bands. It shows that the magnitude has the required accuracy in range $[0,0.0093]$ rad/s and the phase in range $[0,0.0081]$ rad/s. The intersection of these intervals is the range of validity of $G_c(s)$, which is $\omega_{\max}=0.0081$ rad/s.

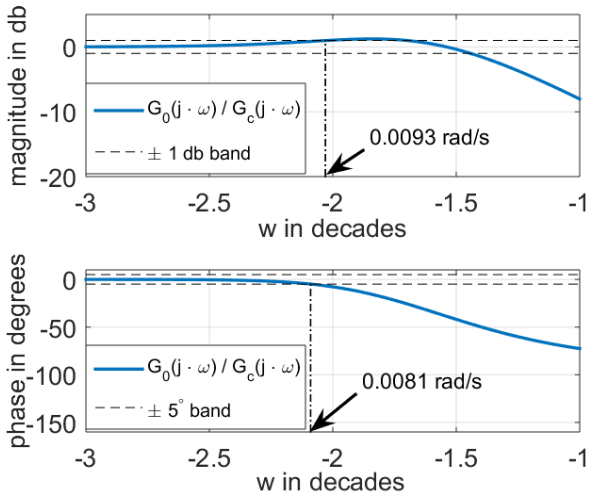

Fig. 3. Frequency response of $G_0(s)/G_c(s)$.

The controller proposed in this paper has the structure:

$$C_\alpha(s) = \frac{K_b \cdot s + K_a}{s^\alpha}, \quad 0 \le \alpha \le 2, \tag{4}$$

where α is the fractional order, which is hereafter denoted the PI^α controller. Note that the *PD* and *PI* controllers are particular cases of (4) when $\alpha = 0$ and $\alpha = 1$ respectively. In order to facilitate the controller design, we impose to cancel the dynamics of $G_c(s)$ on $C_\alpha(s)$:

$$C_\alpha(s) = \frac{K_\alpha \cdot \left((T_{10} + T_{20}) \cdot s + 1\right)}{s^\alpha} = \frac{K_\alpha \cdot \left(98.68 \cdot s + 1\right)}{s^\alpha}, \tag{5}$$

3.2 Control specifications

The controller of the *BZT* is designed according to the simultaneous verification of the following specifications:

1) *A nominal damping condition*. The step response of the nominal closed-loop system (with $P_0(s)$) must do not have overshoot.
2) *A robust settling time condition*. Let us denote t_{s0}, t_{s-} and t_{s+} the closed-loop settling times of $P(s)$ with respectively (2) $\tau = \tau_0$, $\tau = \tau_-$ and $\tau = \tau_+$. It is desired to minimize the maximum value of these three settling times (we reasonably assume that this maximum will be the highest settling time among all the processes included in the range (2)).
3) *A precision condition*. Zero steady state error to a step command, which implies that the controller must include an integral term (of integer or fractional order).

Then the optimization problem given by Specification 2 has to be solved subject to the constraint given by Specification 1. This is expressed as:

$$\min_{\substack{0 \le \alpha \le 2 \\ 0 \le \omega_{c0} \le \omega_{\max}}} \left(\max\left(t_{s0}, t_{s-}, t_{s+}\right)\right), \tag{6}$$

subject to Specification 1, where ω_{c0} is the gain crossover frequency of the nominal open-loop transfer function $L_0(s) = P_0(s) \cdot \mathrm{C(s)}$, which must be included in the validity interval of $G_c(s)$. This last constraint is required in order to guarantee the validity of the approximation (3), that is used to define the controller structure (5). Taking (3) into account, it is verified that:

$$L_0(\mathrm{s}) \approx \frac{K_0 \cdot K_\alpha}{s^\alpha} \cdot e^{-\tau_0 \cdot s} \tag{7}$$

and the gain K_α is tuned for each couple of values (α, ω_{c0}) using the expression:

$$K_\alpha = \frac{\omega_{c0}^\alpha}{K_0} \tag{8}$$

obtained from the condition $\left|L_0(j \cdot \omega_{c0})\right| = 1$ and taking into account that $\left(j \cdot \omega_{c0}\right)^\alpha = e^{j \cdot \frac{\pi}{2} \alpha} \cdot \omega_{c0}^\alpha$.

3.3. Design of a PI controller in the standard control scheme

Fig. 4 shows the standard control scheme in which a *PI* controller is used (hereafter denoted the *PI* control scheme).

The optimization problem (6) is solved for the integral order $\alpha = 1$. The only tunable parameter in (5) is K_α, which is found by a pure search procedure that takes into account constraint 1). It yields an optimum value $\omega_{c0} = 0.00081$ rad/s and a minimum cost of 2450 s. The optimum controller is $C_1(\mathrm{s}) = 0.0027 \cdot (98.68 \cdot \mathrm{s} + 1) / s$. Fig. 5 shows the step responses of that control system for the minimum, nominal and maximum time delays. It is mentioned that in this figure, and the following ones, all the variables are incremental around the operating set point and have been normalized.

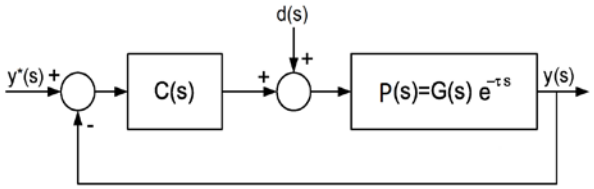

Fig. 4. Standard control scheme.

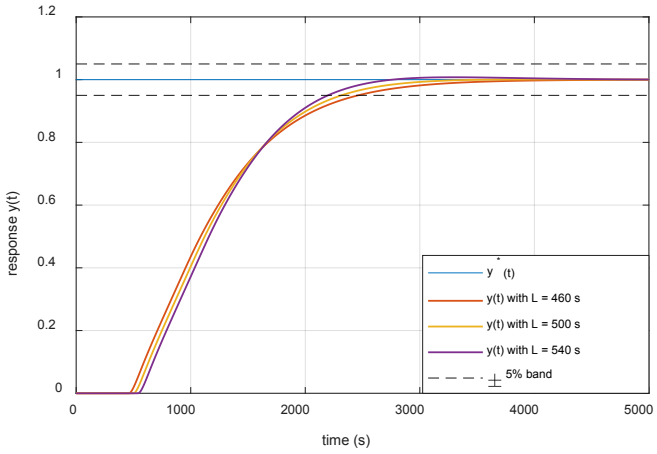

Fig. 5. Step responses of the closed-loop system using a *PI*.

3.3. Design of a PI controller embedded in a SP scheme.

Fig. 6 shows a Smith Predictor control scheme in which a *PI* controller is used (hereafter denoted *SP-PI*).

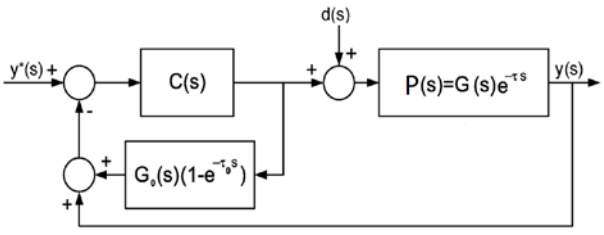

Fig. 6. Smith Predictor based control scheme.

The closed-loop transfer function of our process is:

$$\frac{y(s)}{y^*(s)} = M(s) = \hat{M}(s)\cdot e^{-\tau\cdot s} \tag{9}$$

$$\hat{M}(s) = \frac{C(s)\cdot G_0(s)}{1+C(s)\cdot G_0(s)(1+e^{-\tau\cdot s}-e^{-\tau_0\cdot s})} \tag{10}$$

In the case of the nominal process, $\tau = \tau_0$ and expression (10) becomes $\hat{M}_0(s) = C(s)\cdot G_0(s)/\left(1+C(s)\cdot G_0(s)\right)$.

The optimization problem (6) is solved using a fixed integral order $\alpha = 1$, in which the controller is designed taking into account that now $L_0(\mathrm{s}) \approx K_0\cdot K_\alpha / s^\alpha$. It yields an optimum value $\omega_{c0} = 0.0081$ rad/s, and a minimum cost of 1373 s. The optimum controller is $C_1(\mathrm{s}) = 0.027\cdot(98.68\cdot \mathrm{s}+1)/s$. Fig. 7 shows the step responses of that control system for the minimum, nominal, and maximum time delays. This figure shows that the maximum settling time (the worst case) has been significantly reduced compared to the settling time of the *PI*. Moreover, the response in the case of the nominal process is considered adequate since it does not have overshoot and its settling time is 878 s, which is relatively close to the one of the open-loop response. However, an undesirable 15.7% overshoot appears in the case of the maximum time delay and an undesirable 16.7% undershoot in the case of the minimum time delay.

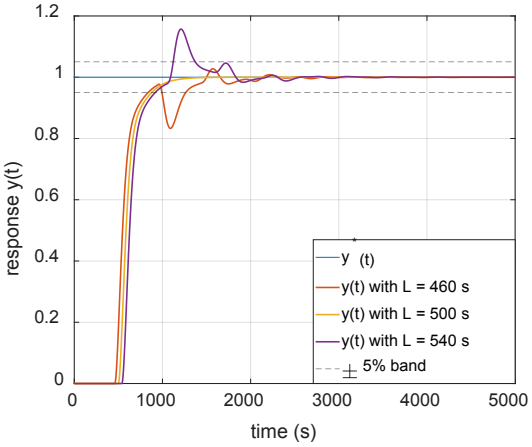

Fig. 7. Step responses of the *SP-PI*.

3.4. Design of a PI^α controller embedded in a SP scheme

In order to reduce these over and undershoots, the Smith Predictor control scheme is combined with the fractional order controller (4), (hereafter denoted $SP-PI^\alpha$). The design of this controller has therefore the following objectives: 1) maintain the nominal response (when the process is $P_0(s)$) obtained with the previous $SP-PI$, 2) the cost index $\max\left(t_{s0}, t_{s-}, t_{s+}\right)$ must be equal or smaller than the optimum cost of 1373 s attained with the $SP-PI$, and 3) the overshoot and undershoot obtained in the previous subsection in the cases of the extreme time delays must be reduced to half their values. In the case of the nominal process $P_0(s)$, the nominal closed-loop transfer function (10) becomes

$$\hat{M}_0^{(\alpha)}(s) = \frac{K_0\cdot K_\alpha}{s^\alpha + K_0\cdot K_\alpha} \tag{11}$$

This transfer function has a slow convergence to its final value if $\alpha < 1$. Then, in order to achieve the same nominal behaviour as the one obtained using the $SP-PI$, the reference $y^*(t)$ is passed through a prefilter which has the form:

$$F(s) = \frac{\hat{M}_0^{(1)}(s)}{\hat{M}_0^{(\alpha)}(s)} = \frac{K_1}{K_\alpha}\frac{s^\alpha + K_0\cdot K_\alpha}{s + K_0\cdot K_1} \tag{12}$$

where we recall that K_1 is K_α for the case $\alpha = 1$. Then a search procedure is carried out in which the pair of values (α, ω_{c0}) are tuned to fulfil objectives 2 and 3 (using again $L_0(\mathrm{s}) \approx K_0\cdot K_\alpha / s^\alpha$). The result of this search is $\alpha = 0.85$, $\omega_{c0} = 0.0027$ rad/s, which yields a controller:

$$C_{0.85}(s) = \frac{0.0219\cdot(98.68\cdot \mathrm{s}+1)}{s^{0.85}}. \tag{13}$$

The closed-loop responses to step commands using prefilter (12) and controller (13) are shown in Fig. 8. This figure shows that the maximum settling time is 1370 s (slightly lower than 1373 s), the overshoot obtained with the maximum time delay is 7.5% and the undershoot with the minimum time delay is 8.4%, which are both about the half of the values obtained with the $SP-PI$ controller. Moreover, these responses are smoother than the ones shown in Fig. 7.

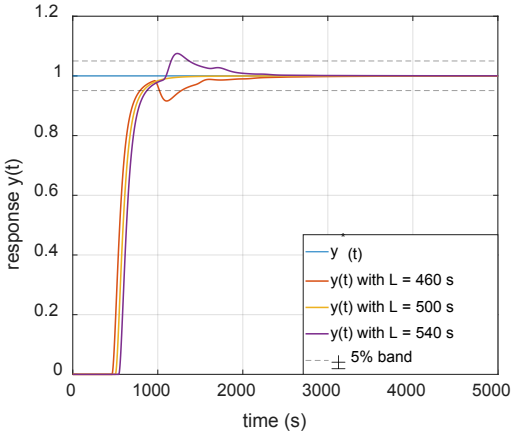

Fig. 8. Step responses of the $SP\text{-}PI^\alpha$.

3.5. Performance analysis.

The performances of the three designed controllers are exhibited in Table I. It shows: 1) the output index $IAE = \int_0^\infty \left|y^*(t) - y(t)\right|\cdot dt$, 2) the maximum amplitude

(*MU*) of the control signal, and 3) the settling time t_s^p of $y(t)$ when a step disturbance is applied to the input of the process. This settling time is the time needed by the output to reduce its error to the 5% of the steady state error that the open-loop system would have as consequence of the step disturbance (i.e, the error caused by the disturbance if a closed-loop control had not been implemented).

4. CONCLUSIONS

Three schemes have been designed for the temperature control of one of the processes of an industrial cement rotary kiln with a large time delay that experiences moderate changes of up to ±8% of its nominal value. The robustness of these three controllers has been assessed and the proposed $SP-PI^{\alpha}$ controller (combined with a prefilter) showed the best performance in terms of settling time and over-undershoot. It is noted that prefilter (12) does not add any degree of freedom to the design of the control system since it is uniquely defined once the parameters α and K_{α} of the closed-loop controller have been tuned. Table I shows the best *IAE* index of the response of the $SP-PI^{\alpha}$ in all the time delay range and that it is achieved with less control effort (less maximum amplitude of the control signal) than the $SP-PI$.

Table I. Performance indexes

Control system	Process	*IAE*	*MU*	t_s^p
PI	τ_-	748.2	3.3	3014
	τ_0	718.3	3.3	2910
	τ_+	693.7	3.4	2834
SP-PI	τ_-	151.9	3.5	1851
	τ_0	115.6	3.3	1499
	τ_+	149.1	4.2	2031
SP- PI^{α}	τ_-	140	3.3	3524
	τ_0	115.4	3.3	3423
	τ_+	136.5	3.7	3308

However, the last column of Table I shows that the $SP-PI^{\alpha}$ has the worst performance when rejecting step disturbances at the input. This feature is caused by having a controller with an integrator of order less than 1, which slows down the convergence of the response to its final value. There are at least two ways of improving this: one is to design a controller (5) with a higher α at the cost of reducing the performance and robustness to a step command, the other is to substitute the term $1/s^{\alpha}$ by $(s+\mu)/s^{1+\alpha}$ in (5), choosing a μ value small enough to do not change the gain crossover frequencies ω_c of the system in the range of time delays (μ is one tenth of the minimum of these ω_c, e.g. Feliu-Batlle et al., 2009).

REFERENCES

Alsop, P.A. (2014). *The Cement Plant Operations Handbook*, 6th ed. Tradeship Publication LTD, Surrey, UK.

Astrom, K., and Hagglund, T. (2009). *Advanced PID Control*. Pearson Education S.A., Madrid, Spain.

Atmaca, A., and Yumrutas, R. (2014). Analysis of the parameters affecting energy consumption of a rotary kiln in cement industry. *Applied Thermal Engineering*, 66, 435–444.

Chen, H., Zhang, X., Hong, P., Hu, H., and Yin, X. (2016). Recognition of the temperature condition of a rotary kiln using dynamic features of a series of blurry flame images. *IEEE Transactions on Industrial Informatics*, 12(1), 148–157.

Fallahpour, M., Fatehi, A., Araabi, B.N., and Azizi, M. (2008). A Neuro-fuzzy controller for rotary cement kilns. *IFAC Proceedings Volumes*, 41(2), 13259–13264.

Feliu-Batlle, V., and Rivas-Perez, R. (2019). Smith predictor based fractional-order integral controller for robust temperature control in a steel slab reheating furnace. *Transactions of the Institute of Measurement and Control*, 1–14.

Feliu-Batlle, V., Rivas-Perez, R., and Castillo-Garcia, F.J. (2009). Fractional order controller robust to time delay variations for water distribution in an irrigation main canal pool. *Computers and Electronics in Agriculture*, 69, 185–197.

Ljung, L. (1999). *System Identification: Theory for de User*. Prentice Hall, New Jersey, USA.

Monje, C.A., Chen, Y.Q., Vinagre, B.M., Xue, D., and Feliu, V. (2010). *Fractional-order systems and controls: fundamentals and applications*. Springer-Verlag, London, UK.

Ravi, T., Sridhar, P., and Guruprasath, M. (2016). Control and optimization of a triple string rotary cement kiln using model predictive control. *IFAC-PapersOnLine*, 49(1), 748–753.

Salcedo, J., Rivas, R., and Sotomayor, J.J. (2018). Design of a generalized predictive controller for temperature control in a cement rotary kiln. *IEEE Latin America Transactions*, 16(4), 1015–1021.

Schneider, M. (2019). The cement industry on the way to a low-carbon future. *Cement and Concrete Research*, 124, 105792.

Sayyaf, N., Tavazoei, M.S. (2018). Robust fractional-order compensation in the presence of uncertainty in a pole/zero of the plant. *IEEE Transactions on Control Systems Technology*, 26(3), 797–812.

Ying, K. (2014). Research on the burning zone temperature control of cement rotary kiln based on CMAC-PID algorithm. *Journal of Chemical and Pharmaceutical Research*, 6(3), 813–817.

Zhang, H. (2017). Application of improved fuzzy-Smith controller in the control system of cement rotary kiln. *Advances in Engineering Research*, 153, 108–112.

Zhou, P., and Meng, Y. (2014). Intelligent dynamic modeling for online estimation of burning zone temperature in cement rotary kiln. In: *Proceeding of the 11th World Congress on Intelligent Control and Automation*, 6167–6171, Shenyang, China.